Article published online: 2023-10-30



# Characterization of the Masquelet Induced Membrane Technique in a Murine Segmental Bone Defect Model

## *Caracterização da membrana induzida pela técnica de Masquelet em modelo murino de defeito ósseo segmentar*

João Antonio Matheus Guimarães[1] Breno Jorge Braga Scorza[2] Jamila Alessandra Perini[1,3] Amanda dos Santos Cavalcanti[4] Maria Eugênia Leite Duarte[5]

[1] Graduate coordinator, National Institute of Traumatology and Orthopedics, Rio de Janeiro, RJ, Brazil
[2] Orthopedic surgeon, Master's Degree in Applied Sciences to the Musculoskeletal System, National Institute of Traumatology and Orthopedics, Rio de Janeiro, RJ, Brazil
[3] Researcher, Research Laboratory in Pharmaceutical Sciences, Universidade do Estado do Rio de Janeiro (UERJ), Rio de Janeiro (RJ) Brazil

Rev Bras Ortop 2023;58(5):e798–e807.

**Address for correspondence** João Antonio Matheus Guimarães, MD, PhD, National Institute of Traumatology and Orthopedics, Av. Brasil, 500, Caju, Rio De Janeiro, RJ, 20940-070, Brasil (e-mail: jmatheusguimaraes@gmail.com).

[4] Researcher, National Institute of Traumatology and Orthopedics, Rio de Janeiro, RJ, Brazil
[5] Researcher at IDOR, Instituto D'Or de Pesquisa e Ensino, Rio de Janeiro, RJ, Brazil

**Abstract**

**Objective** To reproduce in an animal model the surgical technique of Masquelet used in the treatment of critical bone defects and to analyze the characteristics of the membrane formed around the bone cement.

**Methods** A 10mm critical defect was created in the femoral shaft of 21 Sprague-Dawley rats. After resection of the central portion of the diaphysis, the defect was stabilized with a Kirschner wire introduced through the medullary canal and with the interposition of a bone cement spacer. After 2, 4, and 6 weeks of the surgical procedure, the animals were euthanized and evaluated on radiographs of the posterior limb regarding the size of the defect, alignment and stability of the osteosynthesis. The membranes formed around the spacer were subjected to histological analysis to assess thickness, connective tissue maturation and vascular density.

**Results** Over time, the membranes initially made up of loose connective tissue were replaced by membranes represented by dense connective tissue, rich in thick collagen fibers. At six weeks, membrane thickness was greater (565 ± 208µm) than at four

**Keywords**
- bone and bones
- masquelet technique
- models, animal
- membrane induced
- bone regeneration

*Work developed at the National Institute of Traumatology and Orthopedics, Rio de Janeiro, RJ, Brazil.*

**received**
September 23, 2022
**accepted**
December 16, 2022

**DOI** https://doi.org/10.1055/s-0043-1771490.
**ISSN** 0102-3616.



Thieme Revinter Publicações Ltda., Rua do Matoso 170, Rio de Janeiro, RJ, CEP 20270-135, Brazil

(186.9 ± 70.21μm, p = 0.0002) and two weeks (252.2 ± 55.1μm, p = 0.001). All membranes from the initial time showed foci of osteogenic differentiation that progressively reduced over time.

**Conclusion** In addition to the structural and protective function of the membrane, its intrinsic biological characteristics can actively contribute to bone regeneration. The biological activity attributed by the presence of foci of osteogenesis confers to the membrane the potential of osteoinduction that favors the local conditions for the integration of the bone graft.

## Resumo

**Objetivo** Reproduzir em modelo animal a técnica cirúrgica de Masquelet utilizada no tratamento de defeitos ósseos críticos e analisar as características da membrana formada em torno do cimento ósseo.

**Métodos** Um defeito crítico de 10mm foi realizado na diáfise femoral de 21 ratos Sprague-Dawley. Após a ressecção da porção central da diáfise o defeito foi estabilizado com fio de Kirschner introduzido pelo canal medular e com a interposição de espaçador de cimento ósseo. Após 2, 4, e 6 semanas do procedimento cirúrgico os animais foram eutanasiados e avaliados em radiografias do membro posterior quanto ao tamanho do defeito, o alinhamento e a estabilidade da osteossíntese. As membranas formadas em torno do espaçador foram submetidas a análise histológica para avaliação da espessura, da maturação do tecido conjuntivo e da densidade vascular.

**Resultados** Ao longo do tempo as membranas inicialmente constituídas por tecido conjuntivo frouxo foram substituídas por membranas representadas por tecido conjuntivo denso, rico em fibras colágenas espessas. Com seis semanas a espessura das membranas foi maior (565 ± 208μm) do que com quatro (186,9 ± 70,21μm, p = 0,0002) e duas semanas (252,2 ± 55,1μm, p = 0,001). Todas as membranas do tempo inicial apresentaram focos de diferenciação osteogênica que reduziram progressivamente ao longo do tempo.

**Conclusão** Além da função estrutural e protetora da membrana, suas características biológicas intrínsecas podem contribuir ativamente para a regeneração óssea. A atividade biológica atribuída pela presença de focos de osteogênese confere à membrana potencial de osteoindução que favorece as condições locais para a integração do enxerto ósseo.

**Palavras-chave**
- modelos animais
- membrana induzida
- osso e ossos
- regeneração óssea
- técnica de Masquelet

## Introduction

Critical segmental defects are defined as a segmental bone defect with a length 2 to 2.5 times greater than the diameter of the bone that does not regenerate spontaneously.[1,2] Defects with these dimensions are complex lesions that are difficult to approach and represent a challenge for the orthopedist.[3] In animals, a critical bone defect is defined as a defect that does not regenerate spontaneously or that has less than 10% bone regeneration over the life of the animal.[4]

The main therapeutic strategies for critical segmental defects are osteogenic distraction or internal bone transport with an external fixator (Ilizarov technique),[5] vascularized bone grafts[6] and the induced membrane technique described by Alain Masquelet.[7,8]

Initially, Masquelet's surgical technique was described for the treatment of bone loss secondary to infection and began to be progressively used in the reconstruction of critical bone defects. In the technique, performed in two stages, debridement of the lesion is performed with placement of the temporary spacer (cement) in the first stage and, after about six weeks, reconstruction with bone graft is performed.[7,8] The rationale for the technique is based on the formation of a fibrous membrane induced by the foreign body-type inflammatory response around the cement placed at the site of bone resection.[9,10] In the second surgical procedure, the cement is removed and the grafting material is introduced into the chamber formed at the defect site.[11,12]

Reports in the literature have already described the biological properties of the induced membrane that favor consolidation of the defect after bone grafting.[8,13–16] In addition to the mechanical barrier to graft resorption, the membrane is a source of bioactive molecules such as vascular endothelial growth factor (VEGF), responsible for modulating the pattern of membrane vascularization over time,[14,17] and transforming growth factor β1 (TGF- β1), related to the

regulation of proliferation and differentiation of chondrocytes and osteoblasts in the membrane.[15,17–19]

The objective of this study was to reproduce Masquelet's surgical technique in an animal model and to analyze the characteristics of the induced membrane formed around the bone cement over time. In the context of orthopedic research, the model may contribute to (i) identify findings related to the favoring of local conditions for bone consolidation and (ii) enable experiments to be carried out with new materials used for initial filling or in the reconstruction of defects.

## Materials and methods

### Animals

In this study, we used 21 male Sprague-Dawley rats, aged 12-14 weeks, with an average weight of 350 g, acquired at Unicamp's Central Bioterium (Campinas, São Paulo). The animals were housed in an environment with controlled light and temperature and received food and water *ad libitum*. The experiments were carried out in accordance with the guidelines published in Law 11,794 that regulates the procedures for the scientific use of animals and with the approval of the institutional animal care committee (CEUA 006/2017).

### Experimental Model

The surgical procedure was performed after anesthetic induction in a chamber with an alveolar concentration of isoflurane (Biochimico, Itatiaia, Rio de Janeiro) of 4-5%. Then, the animal was transferred to a face mask and maintained at a concentration of 2.5% (Universal Vaporizer, Insight Ltda, Ribeirão Preto, São Paulo). Analgesia was performed with 5 mg/kg of tramadol hydrochloride (Hipolabor, Sabará, Minas Gerais) associated with 5 mg/kg of ketoprofen (Ketoprofen 1%, Vencofarma, Londrina, Paraná) subcutaneously in the preoperative period and maintained at daily for three consecutive days postoperatively. Prophylactic antibiotic therapy was performed with a daily dose of 50 mg/kg of cefazolin sodium (Fazolon®, Blau Farmacêutica, São Paulo) intraperitoneally for three consecutive days. After surgery, the animals were kept individually on ventilated racks.

The surgeries were performed under sterile conditions with the animal in the left lateral decubitus position. After trichotomy and asepsis of the right hind limb with 70% ethanol, a 40-mm longitudinal skin incision was made on the lateral surface of the thigh. After the fascia lata incision, the vastus lateralis muscle was divulsed to expose the right femur (►**Fig. 1A**). To create the defect, a 10 mm ostectomy was performed in the central portion of the femoral

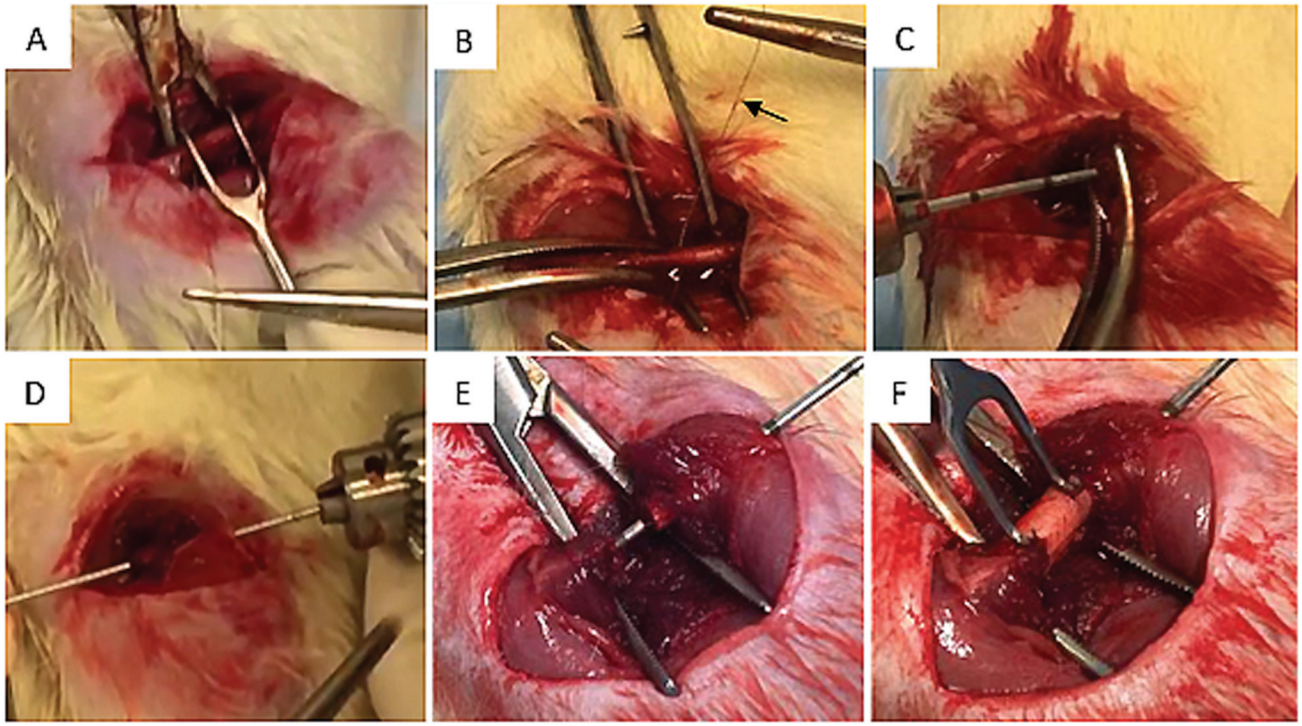


**Fig. 1** Stages of the surgical procedure for creating a critical defect in the femoral shaft in an animal model and reconstruction with bone cement. (**A**) Exposure of the femur by anterolateral access and demarcation of the site for creating the critical defect with a double hook in the mid-diaphyseal portion. (**B**) Ostectomy (10 mm) performed in the central portion of the diaphysis with the aid of a Gigli saw (arrow). (**C**) Insertion of a Kirschner wire (1.5 mm) through the medullary canal of the distal bone segment towards the knee. (**D**) After viewing the end of the wire in the intercondyle fossa, with the aid of a manual motor, the wire was retrogradely progressed through the medullary canal through the bone defect. (**E**) Anchoring of the wire in the trochanteric region of the femur and delimitation of the critical defect. (**F**) Stabilization of the defect with the interposition of a bone cement surgical spacer (PMMA).

diaphysis with the aid of a 0.22 mm Gigli saw (RISystem AG, Landquart, Switzerland) (►**Fig. 1B**).

After resection of the central portion of the diaphysis, a Kirschner wire with a threaded tip and a thickness of 1.5 mm was inserted through the medullary canal of the distal bone segment towards the knee (►**Fig. 1C**). After dislocating the patella and viewing the end of the wire in the intercondyle fossa, with the aid of a manual motor, the wire was retrogradely progressed through the medullary canal through the bone defect (►**Fig. 1D**) and anchored by the thread in the trochanteric region of the femur (►**Fig. 1E**). The size of the flaw was confirmed with a double hook retractor. Stabilization of the defect was obtained with the interposition of a surgical spacer made of bone cement (polymethylmethacrylate, PMMA) prepared in a fume hood with a mixture of 1 g of polymethylmethacrylate with 487 µL of activating liquid (Smartset GMV Endurance, Gentamicin in Bone Cement, DePuy International, Leeds, England). Once the polymerization process had started, the PMMA was molded over the bone defect (►**Fig. 1F**) and, after drying, suturing was performed in layers.

The animals were euthanized two, four and six weeks after surgery with an intravenous injection of a saturated KCl solution under deep inhalation anesthesia. After euthanasia, radiographs of the right hind limb were taken in lateral view to assess the size of the defect, alignment and stability of the osteosynthesis. The size of the bone defects was measured using a radiographic image processing program (mDicomViewer, Microdata version 3.0).

### Histological analysis

After euthanasia, the right hind limb was disarticulated at the hip, the soft tissues were removed and the femur was exposed. The membranes covering the PMMA were removed using tweezers and a scalpel and fixed on filter paper in 10% buffered formalin (pH 7.4). After 48 hours, they were sectioned into longitudinal fragments (►**Fig. 2**), included in paraffin blocks to obtain histological sections 5 µm thick and subsequently stained using the Hematoxylin and Eosin (H&E) technique. Images were obtained on the ApoTome 2 system in a high-resolution AxioCam HRm camera (Zeiss Axiozoom v.16, Carl Zeiss, Munich, Germany) and digitized in the Zeiss Zen 2 core analysis program (Carl Zeiss).

The thickness measurement was obtained at equidistant points along the entire length of the membranes using the Image J software (freely available at https://imagej.nih.gov/ij/). The degrees of connective tissue maturation (loose, dense and very dense) and the vascularity (low, intermediate and high) of the membranes were defined by semi-quantitative evaluation.

### Statistical analysis

Defect sizes and membrane thickness in microns were expressed as mean ± standard deviation and compared using one-way ANOVA followed by Holm-Sidak's post test. Values for $p < 0.05$ were considered significant. Analyzes were performed using GraphPad Prism version 8.3 for iOS (Home-graphpad.com).

**Fig. 2** After fixation in 10% buffered formalin for 48 hours, the membranes were sectioned into equidistant longitudinal fragments, embedded in paraffin and stained using the Hematoxylin-Eosin (H&E) technique.

## Results

### Surgical procedure

The surgeries lasted an average of 32 minutes. Although the animals presented some degree of lameness after recovery from anesthesia, they remained active during the experimental period. At the end of the third day, after suspending the analgesia and antibiotic therapy schemes, the animals recovered the functionality of the operated limb.

### X-ray control

The average size of bone defects was 7 ± 1.5 mm. None of the animals presented displacement of the bone cement or infection at the surgical site. In eighteen animals, osteosynthesis ensured the stability of the bone segments, with good overlapping of the PMMA inserted along the defect (►**Fig. 3**). Three animals that showed signs of osteosynthesis failure due to loss of trochanteric anchoring (►**Fig. 4**) were euthanized and excluded from the study.

### Membrane morphology

In all animals, the membranes completely surrounded the PMMA spacer (►**Fig. 5**). Microscopically, the surface portion in contact with the cement was represented by a densely cellular layer (►**Fig. 6**). Despite the clear delimitation between the cell lining and the upper fibrous portion of the membrane, there was no evidence of the presence of a basement membrane.

Connective tissue density changed over time (►**Table 1**). Within two weeks, the membranes were represented by richly vascularized granulation or connective tissue with deposition of amorphous extracellular matrix related to young fibroblasts (►**Fig. 7A**). From the fourth week, the fibroblasts are elongated and the extracellular matrix acquires a fibrillar appearance (►**Fig. 7B**). At six weeks the

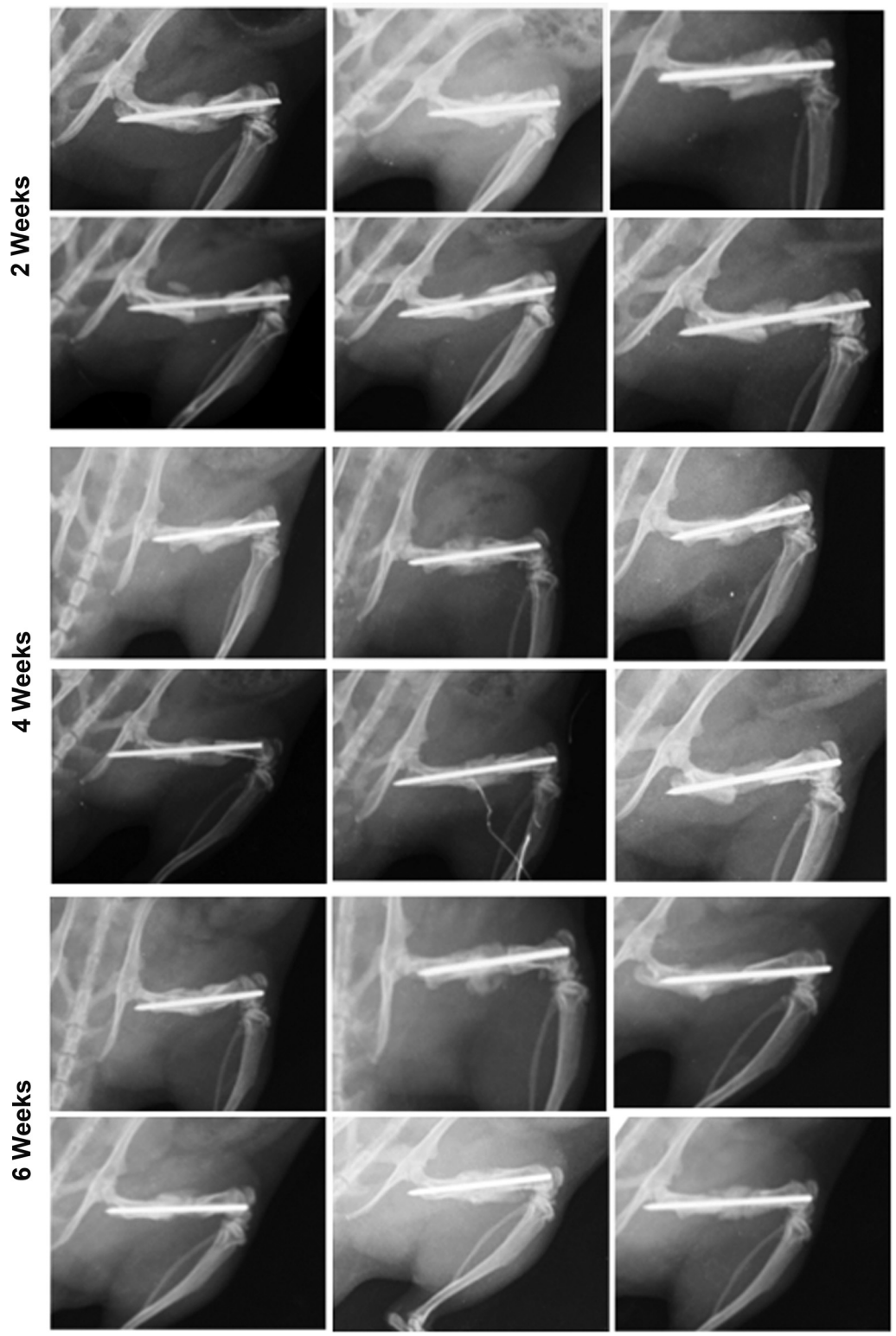


**Fig. 3** Posterior limb radiographs taken after euthanasia to assess defect size, alignment, and osteosynthesis stability. Semanas = Weeks

connective tissue is rich in elongated fibroblasts and dense collagen matrix (►**Fig. 7C**). Except for the slight increase in vessel wall thickness in the later evaluation, the pattern of vascular neoformation showed no relationship with time (►**Table 1**).

The thickness of the membranes increased significantly over time (►**Fig. 8**). At six weeks, the membranes had an average thickness of $565 \pm 208$ µm and, in most animals, the connective tissue penetrated the underlying skeletal muscle, promoting the anchoring of the membrane at the site of the

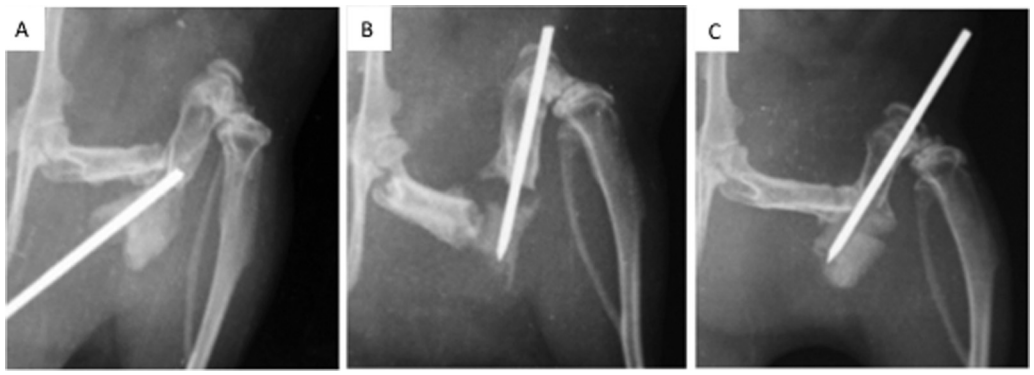


**Fig. 4** Lateral radiographs of the animals that presented failure due to loss of trochanteric anchorage. (**A**) Complete displacement of the Kirschner wire and release of the spacer. (**B** and **C**) Partial displacement of the Kirschner wire with release of the spacer.

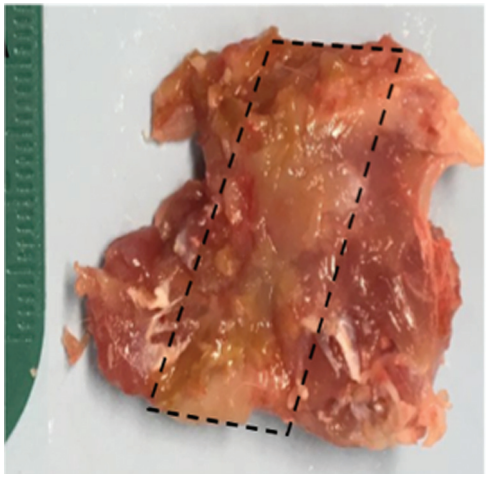

**Fig. 5** Macroscopic aspect of the Masquelet's induced membrane in a murine model with the shiny face related to the polymethylmethacrylate (PMMA) spacer facing upwards (dotted rectangle).

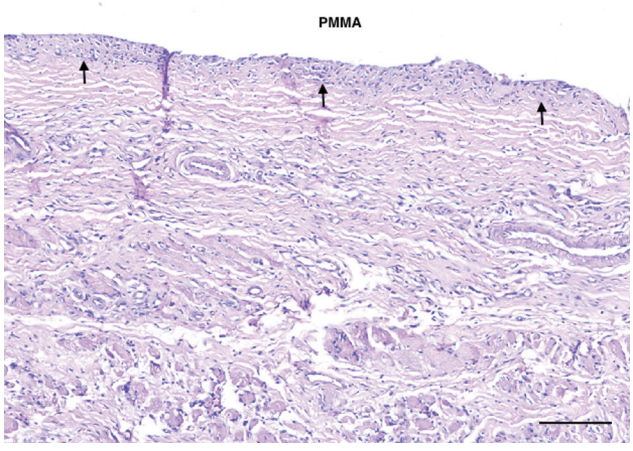


**Fig. 6** Microphotograph of the Masquelet's induced membrane in a murine model four weeks after creation of a critical defect in the femur. Surface coating in contact with the polymethylmethacrylate (PMMA) spacer represented by a densely cellular layer, with a well-defined interface (arrows) on the upper portion of the membrane. H&E Coloring. Bar = 150µm.

**Table 1** Semi-quantitative histological analysis of the degrees of connective tissue maturation and vascular neoformation in the membranes

| Parameter | | 2 weeks (n = 6) | 4 weeks (n = 6) | 6 weeks (n = 6) |
|---|---|---|---|---|
| Membrane connective tissue density | loose<br>dense<br>very dense | 2 (33%)<br>3 (50%)<br>1 (17%) | 0 (0%)<br>4 (67%)<br>2 (33%) | 0 (0%)<br>1 (17%)<br>5 (83%) |
| Vascularization | low<br>intermediate<br>high | 1 (17%)<br>0 (0%)<br>5 (83%) | 1 (17%)<br>0 (0%)<br>5 (83%) | 0 (0%)<br>4 (67%)<br>2 (33%) |

bone defect (►**Fig. 9**). At four and two weeks, the mean thickness was respectively 186.9 ± 70.21 and 252.2 ± 55.1 µm.

As for the intrinsic potential for osteogenic differentiation, all membranes evaluated at the initial time of two weeks (6/6) showed foci of endochondral ossification. Over time, this potential progressively reduced (4/6 at four weeks and 1/6 at six weeks). Regardless of the point of observation, new bone formation occurred in all regions of the membrane, with no definition of a preferred pattern of location (►**Fig. 10**). In some membranes there was an association of newly formed bone with hematopoietic cells.

## Discussion

In this study, we established a murine model of mid-diaphyseal bone defect in the femur with the placement of a retrograde intramedullary nail (threaded Kirschner wire) in order to mimic the Masquelet technique. Animal models that mimic the clinical situation are particularly interesting for testing orthopedic bioengineering strategies based on the development of bone substitutes. In our model, we reproduce membrane formation and show its intrinsic potential for osteogenic differentiation and the organization and maturation of connective tissue over time.

The granulation tissue and extracellular matrix of early-stage membranes becomes progressively denser and richer in thick collagen fibers. In rabbits[19] and sheep[13], structural

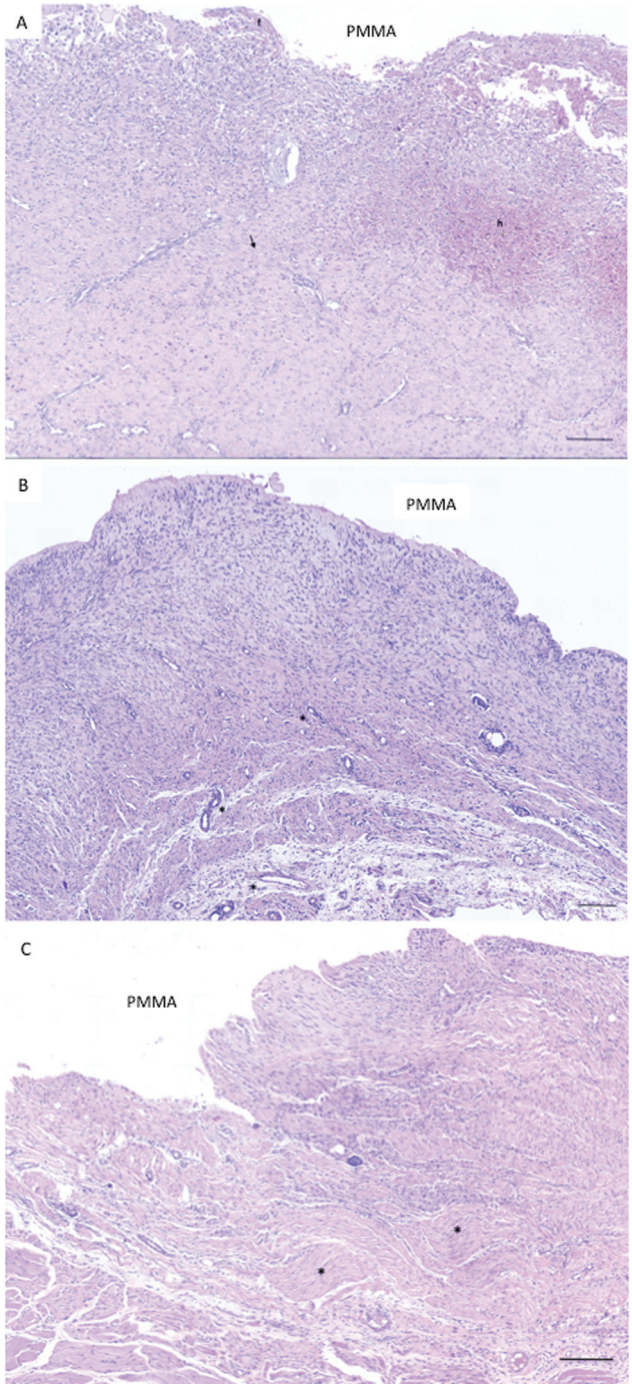


**Fig. 7** Microphotograph of the induced membranes illustrating the characteristics of the fibrous connective tissue two, four and six weeks after the creation of a critical defect in the femur. (**A**) Two weeks: richly vascularized connective tissue associated with amorphous extracellular matrix related to young fibroblasts (arrow), foci of hemorrhage (h) and fibrin deposits (f). (**B**) Four weeks: exuberant vascularization (*) and extracellular matrix with a fibrillar aspect related to fibroblasts with elongated morphology. (**C**) Six weeks: connective tissue rich in fibroblasts trapped in a dense collagen matrix with fibers arranged in parallel (*). PMMA = polymethylmethacrylate. H&E Coloring. Bar = 200µm (A, B and C).

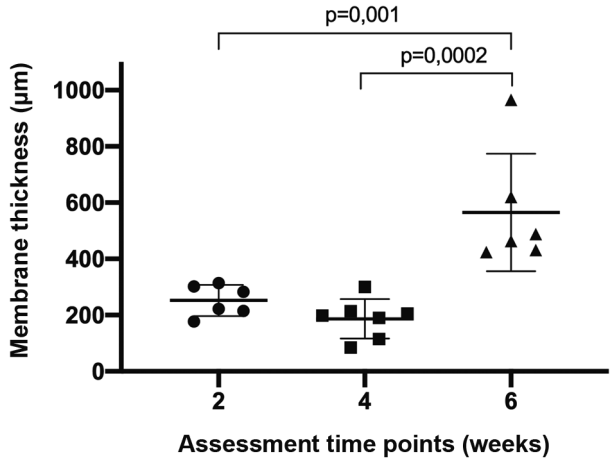


**Fig. 8** Relationship between temporality and membrane thickness. Values expressed as mean ± standard deviation. ANOVA one way followed by Holm-Sidak's post test. Espessura da membrana (µm) = Membrane thickness (µm), Pontos de avaliação (semanas) = Assessment time points (weeks)

changes related to membrane aging were not observed. However, in one of the major clinical studies designed to investigate the biology of membranes, over time, the connective tissue became more collagenized and less vascularized, reaching its final composition three to six months after spacer placement.[14] From the second week after the surgical procedure, we observed the formation of a fibrous membrane surrounding the spacer in all animals. Several reports confirm the morphostructural similarity of the membrane formed around PMMA in humans and animals.[12] In both scenarios it is constituted by well-structured connective tissue organized in layers.[15,20] The surface portion of the membrane in contact with the cement is lined by polyhedral cells arranged in layers, similar to epithelial linings.[8] Subsequent layers are made up of fibroblasts, myofibroblasts, and extracellular matrix rich in type I collagen.[8,15,16,19,21]

Except for the thickening of the vascular wall, we did not observe any influence of time on membrane vascularization. Although vascularization decreases as the membrane becomes more collagenized,[14] it is possible that the comparative evaluation form we used to quantify vessel density did not confirm this finding. A 60% reduction in vascularity from the first to the third month was described in membrane fragments obtained from sequential biopsies performed on the same patient.[14] Another point to be considered is that, in general, the assessment of the vascularization pattern is carried out after the defect has been reconstructed.[20] Possibly bone grafting interferes with the dynamics of membrane remodeling, making it difficult to compare with membranes formed before defect reconstruction.

Reports of membrane thickness in animal models, ranging from 100-200µm[16,20,22,23] to 1000 µm[17,19] are in accordance with the range of values obtained in the present study. Like other authors,[17,18,23,24] we observed that the membranes became thicker over time, which can be explained by the greater accumulation of connective tissue and thick collagen fibers. Studies carried out in rats[22] and rabits[17,20] show that, with time, the membrane becomes thinner. In none of these studies did the authors suggest the biological/biomechanical bases to justify their results. Similar to the pattern of vascularization, it is possible that this discrepancy is related

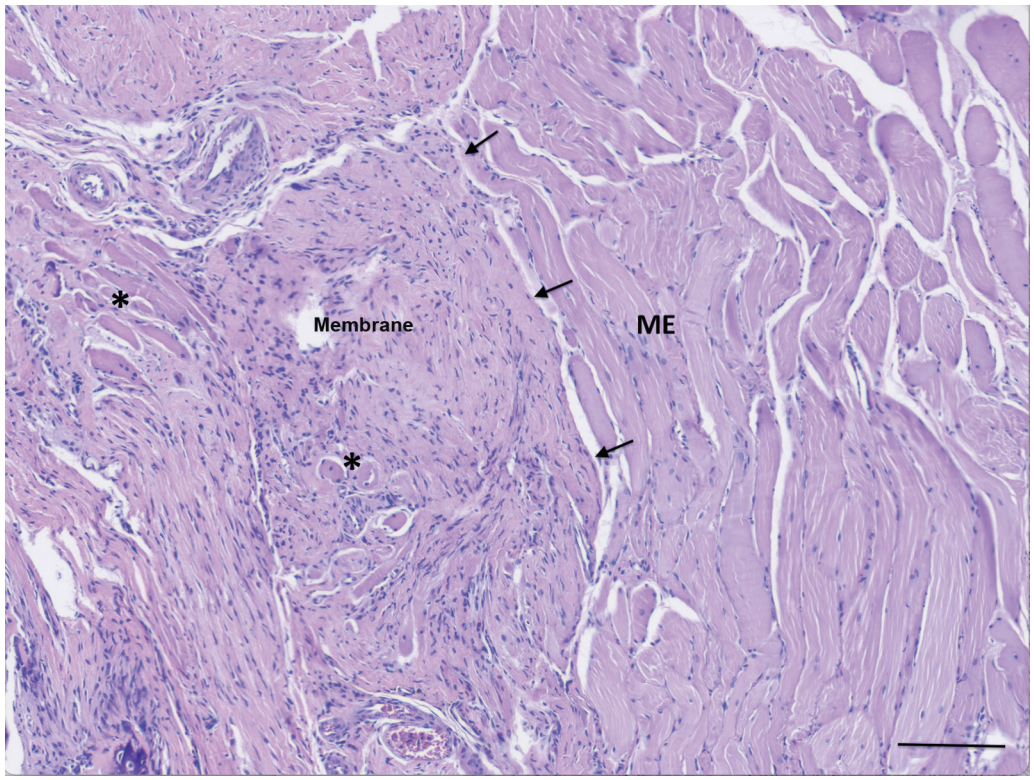


**Fig. 9** In the later evaluation (six weeks) the connective tissue of the membrane (arrows) penetrates the underlying skeletal (ME) muscle promoting the anchoring of the membrane at the site of the bone defect and atrophy of the skeletal muscle fibers (*). PMMA = polymethylmethacrylate. H&E Coloring. Bar = 200µm, Membrana = membrane

to obtaining values for the thickness of the membrane before and after the second surgical procedure. An additional late-observed outcome of our study was the extension of connective tissue from membranes to skeletal muscle. The advantages and disadvantages of local fixation of the membrane may become the subject of future investigations in clinical studies aimed at defining the best time to perform the second surgical procedure of the Masquelet technique.

The intrinsic potential of membranes for osteogenic differentiation demonstrated in the present study and in human[14,25] and animal[16,18] membranes reduced over time.[14,16,18,24,26] The granulation tissue formed in the early stages of the process induced by large foreign bodies is rich in undifferentiated mesenchymal stroma and contains cells that express pluri and multipotentiality markers.[27] This composition confers a high local potential for differentiation in mesenchymal lineages, justifying new bone formation in all membranes evaluated after two weeks. The progressive reduction in the population of mesenchymal progenitors, as the membrane tissue undergoes maturation, would explain the lower percentage of foci of late osteogenesis.

The choice of intramedullary fixation with a Kirshner wire provided mechanical stability at the defect site. There were three fixation failures (3 out of 21 cases), resulting from a technical error in anchoring the wire thread in the trochanteric region of the femur. There are other implants developed for this purpose, but the high cost prevents their use in basic research in our setting. The model proved to be efficient, simple, reproducible and low cost.

A limitation of our study was not having reproduced the second surgical procedure of the Masquelet technique. Another limitation that may be corrected in future studies is the identification of bioactive molecules and mesenchymal progenitors that act in the local regulation of the membrane, using techniques of molecular biology and cell isolation. To ensure the reproducibility of the model, a critical point to be observed during the surgical approach is the maintenance of the space created by the ostectomy until the end of the PMMA polymerization process.

## Conclusion

In addition to the membrane's structural and protective function, its intrinsic biological characteristics can actively contribute to defect healing. The biological activity attributed by the presence of osteogenesis foci confers the osteoinduction potential membrane that favors the local conditions for the integration of the bone graft. The proposed model can contribute to future research aimed at studying this favorable microenvironment that enhances bone regeneration.

Financial Support
The authors declare that they received no financial support from public, commercial or non-profit sources.

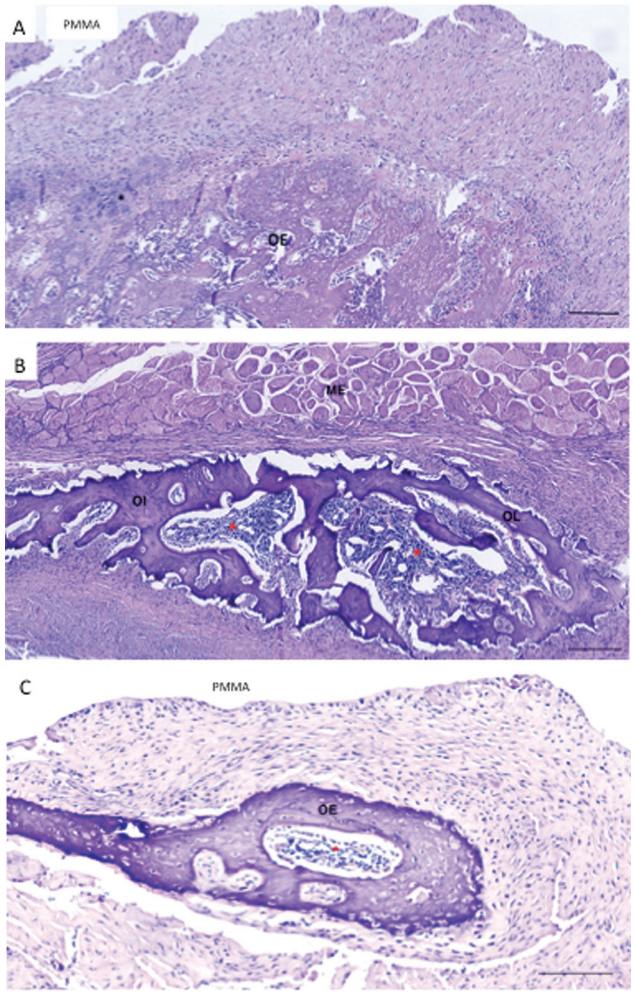


**Fig. 10** Intrinsic potential of membranes to induce osteogenic differentiation. (**A**) Focus of endochondral ossification (OE) located close to the surface of the membrane. Proliferative and hypertrophic chondrocytes (*) can be identified in relation to bone formation (two weeks). (**B**) Focus of ossification located close to the muscular plane consisting of lamellar bone (OL) and immature non-lamellar bone (OI) and hematopoietic cells (*) (4 weeks). (**C**) Focus of endochondral ossification (OE) located close to the surface of the membrane consisting of immature bone containing osteoblasts trapped in the bone matrix and hematopoietic cells (*). PMMA = polymethylmethacrylate. ME = Skeletal muscle. H&E Coloring. Bar = 100µm (A and B) and 50µm (C).

### Conflict of interests

The authors have no conflict of interest to declare.

## References

1 Wiese A, Pape HC. Bone defects caused by high-energy injuries, bone loss, infected nonunions, and nonunions. Orthop Clin North Am 2010;41(01):1–4
2 Mauffrey C, Giannoudis PV, Conway JD, Hsu JR, Masquelet AC. Masquelet technique for the treatment of segmental bone loss have we made any progress? Injury 2016;47(10):2051–2052
3 Kadhim M, Holmes L Jr, Gesheff MG, Conway JD. Treatment options for nonunion with segmental bone defects: systematic review and quantitative evidence synthesis. J Orthop Trauma 2017;31(02):111–119
4 Rimondini L, Nicoli-Aldini N, Fini M, Guzzardella G, Tschon M, Giardino R. In vivo experimental study on bone regeneration in critical bone defects using an injectable biodegradable PLA/PGA copolymer. Oral Surg Oral Med Oral Pathol Oral Radiol Endod 2005;99(02):148–154
5 Giannoudis PV. Treatment of bone defects: Bone transport or the induced membrane technique? Injury 2016;47(02):291–292
6 Ren GH, Li R, Hu Y, Chen Y, Chen C, Yu B. Treatment options for infected bone defects in the lower extremities: free vascularized fibular graft or Ilizarov bone transport? J Orthop Surg Res 2020;15(01):439–450
7 Masquelet AC, Fitoussi F, Bégué T, Muller GP. Reconstruction des os longs par membrane induite et autogreffe spongieuse. Ann Chir Plast Esthet 2000;45(03):346–353
8 Masquelet AC, Begue T. The concept of induced membrane for reconstruction of long bone defects. Orthop Clin North Am 2010;41(01):27–37
9 Masquelet A, Kanakaris NK, Obert L, Stafford P, Giannoudis PV. Bone repair using the Masquelet technique. J Bone Joint Surg Am 2019;101(11):1024–1036
10 Alford AI, Nicolaou D, Hake M, McBride-Gagyi S. Masquelet's induced membrane technique: Review of current concepts and future directions. J Orthop Res 2021;39(04):707–718
11 Giannoudis PV, Harwood PJ, Tosounidis T, Kanakaris NK. Restoration of long bone defects treated with the induced membrane technique: protocol and outcomes. Injury 2016;47(Suppl 6):S53–S61
12 Klein C, Monet M, Barbier V, et al. The Masquelet technique: Current concepts, animal models, and perspectives. J Tissue Eng Regen Med 2020;14(09):1349–1359
13 Pelissier P, Masquelet AC, Bareille R, Pelissier SM, Amedee J. Induced membranes secrete growth factors including vascular and osteoinductive factors and could stimulate bone regeneration. J Orthop Res 2004;22(01):73–79
14 Aho OM, Lehenkari P, Ristiniemi J, Lehtonen S, Risteli J, Leskelä HV. The mechanism of action of induced membranes in bone repair. J Bone Joint Surg Am 2013;95(07):597–604
15 Christou C, Oliver RA, Yu Y, Walsh WR. The Masquelet technique for membrane induction and the healing of ovine critical sized segmental defects. PLoS One 2014;9(12):e114122
16 Gourón R, Petit L, Boudot C, et al. Osteoclasts and their precursors are present in the induced-membrane during bone reconstruction using the Masquelet technique. J Tissue Eng Regen Med 2017;11(02):382–389
17 Wang X, Wei F, Luo F, Huang K, Xie Z. Induction of granulation tissue for the secretion of growth factors and the promotion of bone defect repair. J Orthop Surg Res 2015;10(01):147
18 Henrich D, Seebach C, Nau C, et al. Establishment and characterization of the Masquelet induced membrane technique in a rat femur critical-sized defect model. J Tissue Eng Regen Med 2016;10(10):E382–E396
19 Viateau V, Bensidhoum M, Guillemin G, et al. Use of the induced membrane technique for bone tissue engineering purposes: animal studies. Orthop Clin North Am 2010;41(01):49–56
20 Liu H, Hu G, Shang P, et al. Histological characteristics of induced membranes in subcutaneous, intramuscular sites and bone defect. Orthop Traumatol Surg Res 2013;99(08):959–964
21 Viateau V, Guillemin G, Calando Y, et al. Induction of a barrier membrane to facilitate reconstruction of massive segmental diaphyseal bone defects: an ovine model. Vet Surg 2006;35(05):445–452
22 Gruber HE, Gettys FK, Montijo HE, et al. Genomewide molecular and biologic characterization of biomembrane formation adjacent to a methacrylate spacer in the rat femoral segmental defect model. J Orthop Trauma 2013;27(05):290–297
23 Tang Q, Tong M, Zheng G, Shen L, Shang P, Liu H. Masquelet's induced membrane promotes the osteogenic differentiation of bone marrow mesenchymal stem cells by activating the Smad and MAPK pathways. Am J Transl Res 2018;10(04):1211–1219
24 Nau C, Seebach C, Trumm A, et al. Alteration of Masquelet's induced membrane characteristics by different kinds of antibiotic

enriched bone cement in a critical size defect model in the rat's femur. Injury 2016;47(02):325–334

25 Gruber HE, Ode G, Hoelscher G, Ingram J, Bethea S, Bosse MJ. Osteogenic, stem cell and molecular characterisation of the human induced membrane from extremity bone defects. Bone Joint Res 2016;5(04):106–115

26 Gruber HE, Riley FE, Hoelscher GL, et al. Osteogenic and chondrogenic potential of biomembrane cells from the PMMA-segmental defect rat model. J Orthop Res 2012;30(08):1198–1212

27 Patel J, Gudehithlu KP, Dunea G, Arruda JAL, Singh AK. Foreign body-induced granulation tissue is a source of adult stem cells. Transl Res 2010;155(04):191–199